Cardiac Assist

Near Field Flow Characteristics of the Bjork-Shiley Monostrut Valve in a Modified Single Shot Valve Chamber

Keefe B. Manning,* T. Michael Przybysz,* Arnold A. Fontaine,* John M. Tarbell,† and Steven Deutsch*

In certain mechanical heart valves, cavitation has been shown to develop during closure and rebound, leading to valve damage, blood damage, and strokes. Whereas it is uncertain what causes mechanical heart valve related strokes, some evidence suggests that stable bubbles may be the culprits. Previous work has indicated that vortex cavitation may contribute to stable bubble growth. Therefore, in an effort to understand the vortex cavitation, laser Doppler velocimetry data are collected in a plane parallel to and 3 mm away from the major orifice during closure and rebound of a Bjork-Shiley Monostrut mechanical heart valve. A modified single shot chamber is used that incorporates a more realistic near valve geometry than those used in previous studies. The results show the formation of a vortex during closure, which intensifies during rebound and dissipates during the final closing cycle. A regurgitant jet with mean velocities up to 3 m/s through the clearance gap of the valve provides energy to the vortex. During the final closing cycle, the vortex breaks up into asymmetrical, small scale flow patterns. This study provides further evidence that stable bubble formation may stem from the intense vortex cavitation occurring during valve closure and rebound. *ASAIO Journal* 2005; 51:133–138.

Should a native heart valve need to be replaced because of incompetence or disease, a mechanical heart valve (MHV) is typically selected. There have been more than 1,000,000 mechanical heart valves implanted to replace diseased ones worldwide.[1] Even though they are considered acceptable for human implantation, problems such as strokes and thromboemboli still arise, so MHV patients still undergo anticoagulation management.[2] The range for thromboemoblic rates for bileaflet and tilting disc MHVs is 0.6–6.5% and 1.5–4.7% per patient year, respectively.[3,4] Strokes result from the lodging of a particle (gaseous or solid), or thromboembolism, in a cranial vessel blocking the circulation. The exact cause of MHV related strokes remains unknown because it is difficult to determine whether the particles are solid or gaseous. One potential cause may be the development of cavitation during mechanical heart valve closure. Cavitation has been widely implicated as one of the causes of mechanical heart valve damage with evidence of pitting and structural occluder damage after explantation of mechanical heart valves.[5] Furthermore, cavitation shows a propensity to induce elevated levels of hemolysis and platelet activation, while also producing markedly increased levels of plasma free hemoglobin.[6–8] *In vitro* studies have shown that valves may develop cavitation, with some experiencing higher degrees of cavitation than others.[9–11] There is evidence that suggests that cavitation occurs *in vivo*, but this may not be the case for every MHV. Studies have been conducted in an artificial heart and single shot chamber environment to illustrate cavitation development. These studies have used techniques such as high speed videography and high frequency pressure signals to show cavitation formation.[12–17] Even though these techniques illustrate the development of cavitation, the exact mechanisms for cavitation have yet to be ascertained in regard to MHVs. Certainly, the localized flow field plays an integral role in cavitation, but it is not the sole component. Nuclei must be present to propagate cavitation growth. These may be in the form of minute gas bubbles floating freely within the fluid, gas trapped on the surface of motes or foreign bodies, or gas trapped on the surface of the valve. The number of nuclei may be highest right after valve replacement surgery.

Cavitation develops because of a local pressure drop at or below the vapor pressure of the fluid while at a constant temperature. Local flow fields of MHVs have been implicated in the development of cavitation through water hammer, squeeze flow, regurgitant jets, and vortices during valve closure and rebound.[11,12,18–20] During cavitation growth, dissolved gases may diffuse into the cavities. As the local pressure recovers, the cavities collapse. Noncondensable gases (CO_2, N_2, and O_2) that are released during the cavitation process have to be reabsorbed by the solution, a process that requires much more time than vapor collapse. This leads to the production of long lived, stable bubbles[15–17] shown *in vitro* through an artificial heart and single shot mechanical heart valve chamber. *In vivo*, these stable bubbles may appear in the cranial circulation as high intensity transient signals (HITS) or microembolic signals through transcranial Doppler ultrasound.[21–23] Evidence suggests that HITS may cause strokes or neurologic deficits[24] and that these HITS are actually gaseous and not solid.[25] Droste *et al.*[25] showed that, when patients are placed on pure O_2 after MHV implantation, the number of HITS that are recorded decreases substantially. As noted, these stable bubbles are believed to develop when gaseous nuclei

From the *Department of Bioengineering, The Pennsylvania State University, University Park; and the †Department of Biomedical Engineering, The City College of New York, New York.

Submitted for consideration July 2004; accepted for publication in revised form November 2004.

Reprint Requests: Dr. Steven Deutsch, Department of Bioengineering, The Pennsylvania State University, 205 Hallowell Building, University Park, PA 16802.

DOI: 10.1097/01.MAT.0000153496.01522.E4

that are present in blood flow into low pressure regions associated with valve closure. As the valve closes and rebounds, inducing vaporous cavitation, gas diffuses into the nuclei enlarging the bubble. When the pressure recovers and the vapor collapses, the bubble dynamics and local fluid mechanics prevent the gas from diffusing back into solution, causing the bubble to stabilize and allowing it to flow freely in the vasculature. By stabilizing the nuclei, N_2 and CO_2 have both been suggested as the link to MES/HITS/stable bubble formation,[15–17,26] but there has yet to be concrete proof of this.

The local flow fields are of particular importance to cavitation. With a vortex, cavitation can occur in its low pressure core. Vortex formation has been shown to occur with a tilting disc valve (Bjork-Shiley Monostrut [BSM]) and bileaflet valve (St. Jude Medical) in a single shot chamber using particle image velocimetry.[27–29] The vortex formed with the BSM valve occurred along the major orifice during the closing cycle. With the St. Jude valve, two vortices developed upstream of the valve along a plane perpendicular to the B-datum plane. In these earlier experiments, however, the atrial and ventricular sides of this single shot chamber had a sudden expansion from the mechanical heart valve, with data collected approximately 3–5 mm away from the valve seat. In the current study, we have modified the single shot mechanical heart valve chamber to include more confined regions (similar to sinuses found *in vivo*) on the upstream and downstream sides of the valve. A more realistically confined region may lead to increase vortex strength. Thus we have been able to use laser Doppler velocimetry to obtain results approximately 3 mm from the valve housing to better show the development of the vortex during valve closure and rebound. The aim of this study is to more completely understand the local fluid mechanics that occur during MHV closure and rebound, including the influence of the regurgitant jet and its relation to cavitation development.

Materials and Methods

A 29 mm Bjork-Shiley Monostrut mechanical heart valve with a Pyrolytic carbon occluder was placed in a "single shot" heart valve chamber (**Figure 1**) to simulate the mitral valve closure dynamics. This chamber was modified from previous experiments[27] by including a more confined expansion/contraction on the upstream and downstream sides of the MHV. The expansion/contraction (sinus area) increases to an inner diameter of approximately 40 mm on either side of the MHV. This approach, although not completely anatomically correct, provides a physical limitation for the flow similar to one found *in vivo* (left atrium and left ventricle). The single shot chamber includes a sealed ventricular chamber and an atrial chamber exposed to the atmosphere. The entire chamber was constructed of acrylic for optical accessibility to laser Doppler velocimetry (LDV). The sewing cuff was removed from the valve and replaced with a rubber O-ring. The chamber constructed to hold the BSM valve in place was manufactured from two pieces of acrylic such that, when joined together, a slot was created for the valve. The chamber does not simulate flow through conditions but rather simulates only the MHV closing phase.

A pneumatic pump pressurized the sealed ventricular chamber, forcing the valve to close. The ventricular pressure was measured by a Millar Instruments pressure catheter (Houston, TX) and was used to calculate dP/dt, as described by the Food and Drug Administration (FDA), as the rise in pressure during the 20 ms just before impact. A dP/dt equal to 3,500 mm Hg/s was used to assess the extent of cavitation. To achieve this dP/dt, the pneumatic pump parameters were set for a heart rate of 75 beats per minute (bpm), a systolic duration of 300 ms, and a ventricular pressure of 175 mm Hg. These conditions are known to induce cavitation because the physiologic range for dP/dt (1,500–3,500 mm Hg/s) has produced cavitation.[9,12,17,30] The modified single shot chamber was filled with mineral oil (Penreco Inc, Karns City, PA) that has a specific gravity of 0.825, a viscosity of 4.69 cP, and a refractive index of 1.46. Polystyrene particles, approximately 10 μm in diameter with a specific gravity of 1.1, were added to the fluid for LDV seeding.

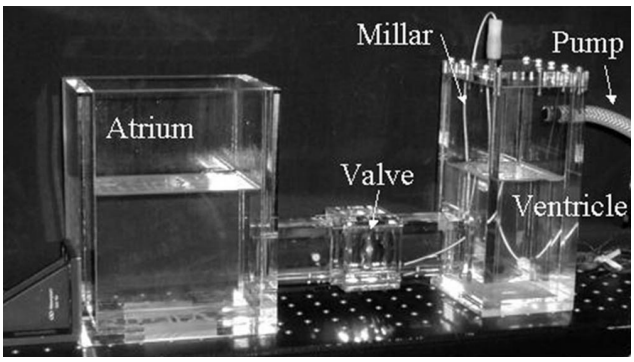

Figure 1. Modified single shot valve chamber.

A two-dimensional LDV system (TSI Inc., St. Paul, MN) obtained the velocities near the major orifice of the BSM MHV. LDV is a noninvasive flow measurement system that provides excellent spatial and temporal resolution. The LDV system uses fiber probes and collects data in the back scatter mode. Two pairs of coherent, collimated laser beams of known wavelengths (green and blue light) are focused to a point. This point is the overlapping of four laser beams creating a measurement

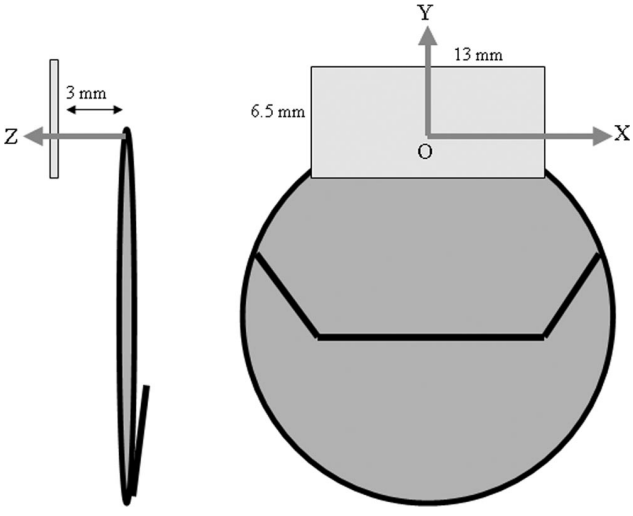

Figure 2. Laser Doppler velocimetry measurement plane and location.

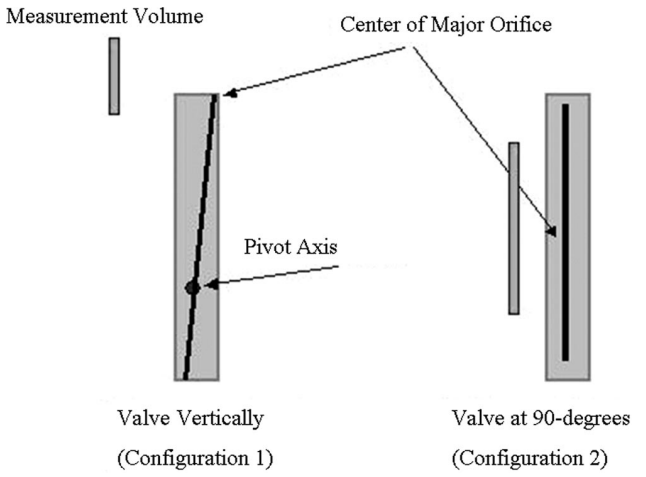

Figure 3. Valve configuration during laser Doppler velocimetry data acquisition.

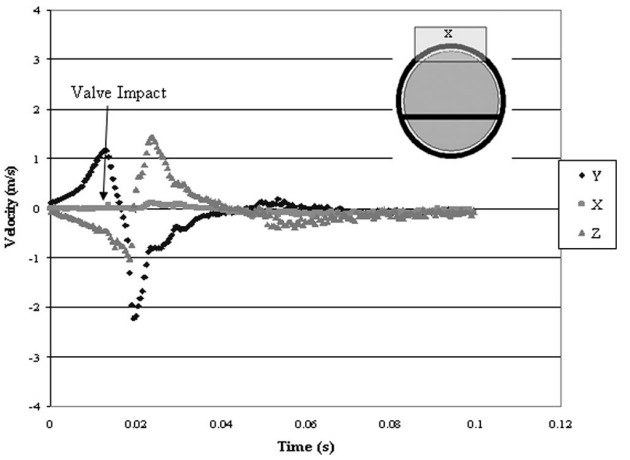

Figure 4. Time history of each velocity component starting before valve closure. X = 0.0 mm, Y = 1.5 mm, and Z = 3.0 mm.

or probe volume. Data were collected in coincident mode (~2,000 measurements), ensuring that particles were measured through each laser within the probe volume at the same time. As illustrated in **Figure 2**, the LDV was used to measure velocities three millimeters upstream from the valve housing on an area of 6.5 × 13 mm surrounding the major orifice. Data were collected every 500 μm within this measurement plane, that is, at 378 locations. The measurement plane was as close to the valves as the Plexiglas curvature would allow. With the major orifice of the valve in the 12:00 position, the x and z components of velocity were captured. The valve was then rotated 90° to capture the y component of velocity and, as a result, verify the z component. This is shown in **Figure 3**. For these data, pseudo-three-dimensional plots of velocity components were reconstructed. Phase window averaging was used to examine the flow fields during the closing phase of the cycle, which included occluder impact and rebound. This technique takes velocity data acquired over a known cycle multiple times and then divides the cycle into distinct time segments to examine velocity data during specified phases.

Results and Discussion

Figures 4 to 6 illustrate the three components of velocity during the MHV closing phase with phase averaging over 1 ms time bins at three different locations 3 mm upstream from the valve housing. The three locations were 1.5 mm above the valve clearance gap, at the clearance gap (0 mm), and 1.5 mm below the clearance gap. Valve impact is indicated in each figure.

Examining the x component (flow moving horizontally across the valve) of velocity, the regions above and at the major orifice do not show a major flow in that direction, as illustrated in **Figures 4 and 5**. However, in **Figure 6**, just below the clearance gap at the major orifice, the mean x component of flow moves in the negative direction and then briefly reverses direction before slowly decaying to near zero mean flow. In the vertical or y component of **Figures 4 to 6**, as the pressure rises in the ventricular chamber and the valve closes, the flow reverses itself before impact. The largest magnitude change occurs 1.5 mm above the major orifice. A second peak in reverse flow occurs at and below the gap. This may be attributed to valve rebound and the regurgitant jet formed. Finally, in the axial or z component, the flow in **Figure 4** moves towards the valve until impact occurs, whereby there is a sudden change in flow direction toward the atrium, with the mean velocity reaching up to 1.5 m/s. The flow then decreases and changes direction again. Similarly, **Figure 5** demonstrates that the flow changes direction at valve impact. However, unlike in **Figures 4 and 5**, **Figure 6** shows no sudden change in mean flow direction after impact but instead includes two more peaks in velocity. At 20 ms after impact, the flow at all three locations has a near zero velocity. Because this chamber does not produce a net flow through the valve, a persistent regurgitant jet does not develop after final valve closure.

Figures 7 to 10 show the three velocity components of the average flow field during closure. The vectors represent the x and y components of velocity, and the color contours represent the z component or axial flow. The origin (0,0) is located in the clearance gap, as mentioned previously. The black arc in **Figures 7 to 10** represents the valve's titanium housing along the major orifice. As the pressure rises in the ventricular cham-

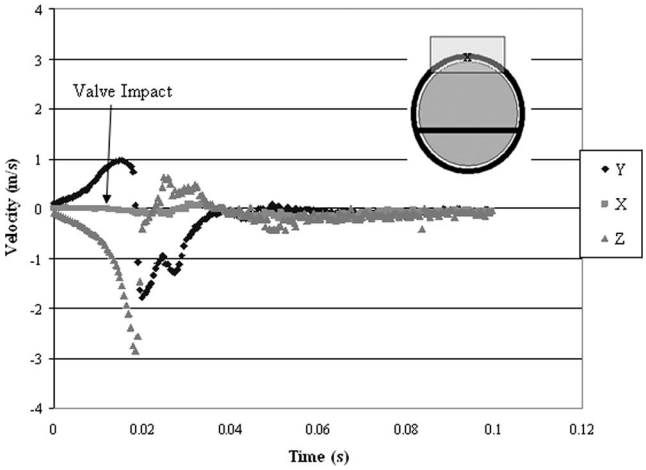

Figure 5. Time history of each velocity component starting before valve closure. X = 0.0 mm, Y = 0.0 mm, and Z = 3.0 mm.

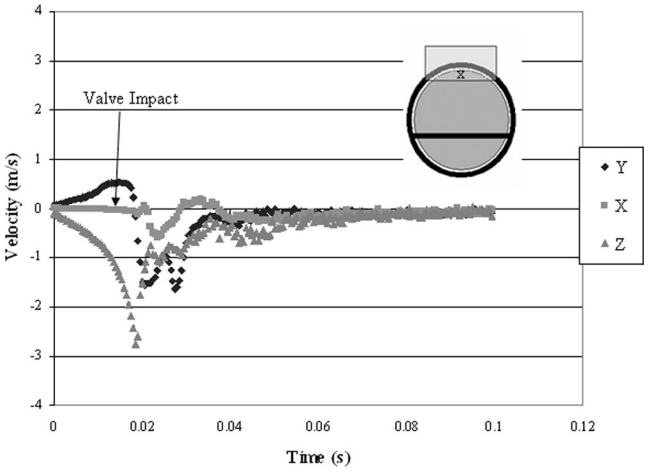

Figure 6. Time history of each velocity component starting before valve closure. X = 0.0 mm, Y = −1.5 mm, and Z = 3.0 mm.

ber, the valve begins to close, but fluid continues to move from the atrium into the ventricle, a closing volume. In these figures, the valve closes toward the reader, as viewed from the atrium. However, approximately 4 ms before impact (**Figure 7**), the axial flow above the valve (black arc) changes direction because of the closing volume reverse flow with velocities increasing in the region of the occluder. This closing volume reverse flow is a form of regurgitant flow that typically occurs during leaflet closure and naturally occurs in both native and manufactured valves. The axial velocity magnitudes increase both above and below the valve housing before impact. The x-y velocities show cross-flow in a mostly vertical direction, converging centrally at nearly 1 m/s. The flow before impact indicates that a recirculation zone has been formed upstream of the valve in the sinus area, a constrained region upstream and downstream of the valve, whereby the acrylic expands to approximately 40 mm. This can be seen from **Figure 11**, whereby the flow (vortex) rotates about a point further upstream than the measurement plane.

Once impact has occurred (**Figure 8**), the axial flow splits along the housing (black arc) and peaks 2 mm above the valve housing, with flow above this arc moving mostly upstream towards the atrium and approaching velocities of 2 m/s and flow below this arc moving almost entirely toward the valve at 2 m/s. Most of the flow above the arc moves vertically downward with high velocities until reaching the arc where the flow reaches the high axial flow component and is redirected towards the valve. The x-y flow below the housing has low velocity magnitudes, suggesting that the driving flow is axial. The vortex formed during closure, as illustrated in **Figure 11**, tightens through an increase in rotation enhanced by the major orifice's regurgitant jet. This three-dimensional vortex, formed immediately after valve closure, is consistent with previous results using particle image velocimetry (PIV). Secondary structures, in the form of large scale recirculation regions that developed early in the closing cycle, mask the averaged picture of the small vortex.

As shown in **Figure 9**, 4 ms later, during valve rebound, the regurgitant jet from the major orifice increased to near peak velocity, with most of the flow in the axial direction above the valve housing moving away from the valve with velocities approaching 2.5 m/s. The jet increased in magnitude as the left ventricular pressure continued to increase in conjunction with the valve closing forcing flow through the clearance gap at the tip of the valve. The peak mean velocity is much lower than the actual velocity because of the phase window averaging over 4 ms. The vortex formed appears to translate closer to the valve, indicated by the downward secondary flow patterns moving into the measurement plane. The vortex illustration in **Figure 11** shifted towards the valve during this time frame. All of the flow at this point in the cycle is moving downward and diverging away from the center of the imaged plane. **Figure 9** represents valve rebound, which is approximately 4–6 ms after impact under these conditions. During impact and rebound, large velocity gradients developed, as observed by the high concentration of narrow axial bands over 3 mm and velocities spread over 3 m/s.

Figure 10 (4 ms later) illustrates this continuing regurgitant flow field after valve rebound when the occluder remained closed and the diverging flow pattern away from the center of

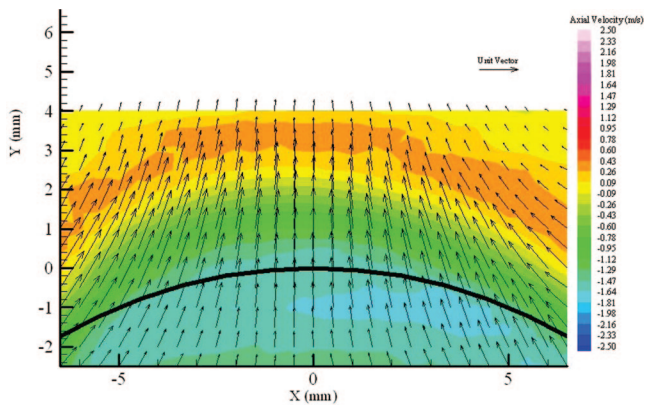

Figure 7. Three-dimensional averaged velocity map of the major orifice regurgitant flow in a Bjork-Shiley Monostrut mechanical heart valve 3 mm away from the valve. The colored contour is the axial velocity, and the vectors represent X and Y velocities. Time = 4 ms before impact.

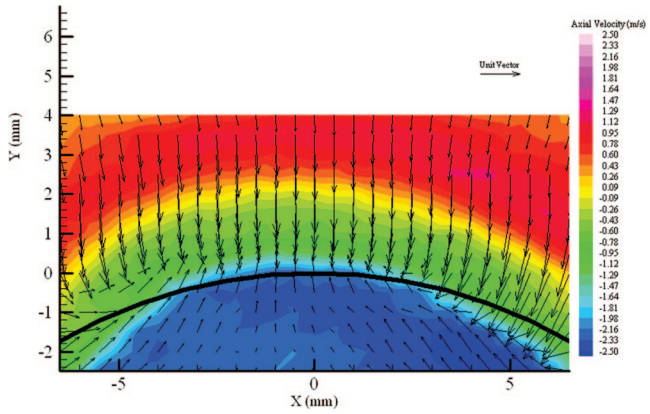

Figure 8. Three-dimensional averaged velocity map of the major orifice regurgitant flow in a Bjork-Shiley Monostrut mechanical heart valve 3 mm away from the valve. The colored contour is the axial velocity, and the vectors represent X and Y velocities. Time = impact.

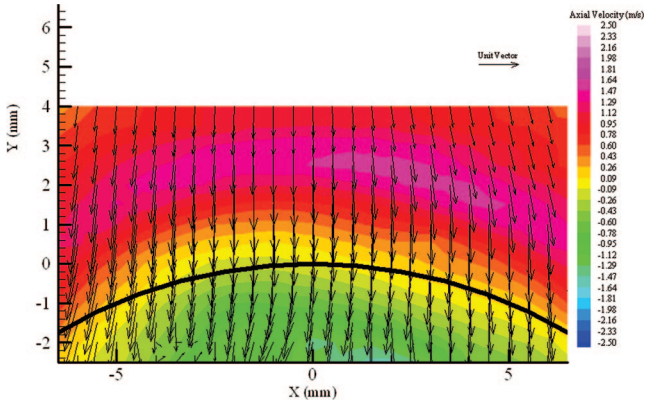

Figure 9. Three-dimensional averaged velocity map of the major orifice regurgitant flow in a Bjork-Shiley Monostrut mechanical heart valve 3 mm away from the valve. The colored contour is the axial velocity, and the vectors represent X and Y velocities. Time = 4 ms after impact.

the imaged plane. A double recirculating pattern moving away from the major orifice was developing, whereas the overall velocity magnitudes decreased. The flow remained symmetrical until nearly 18 ms after rebound, whereby asymmetrical flow characteristics developed. Because this is a single shot chamber with no flow through, the flow subsided, causing minor instability eventually leading into the next cycle.

The overall flow patterns of the BSM mechanical heart valve in this more confined flow chamber further illustrates the nature of a vortex being generated during valve closure. **Figure 12** illustrates the progressive flow behavior before, during, and after valve closure. As the valve began to close, the flow exited the atrial chamber and moved into the ventricular chamber. During this closure phase, a vortex began to form near the major orifice side of the valve and became stronger as the valve approached impact. Once the valve reached impact, a tight vortex near the valve was formed with a regurgitant jet feeding the circulation. During rebound, the vortex and regurgitant jet lost their strength. Finally, at the end of closure, a weak side vortex developed and quickly dissipated. Similar

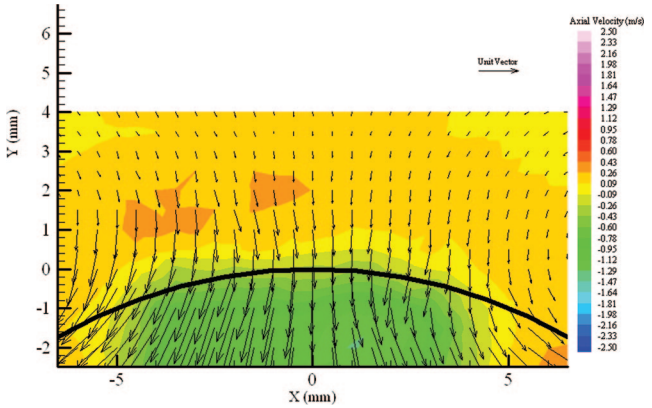

Figure 10. Three-dimensional averaged velocity map of the major orifice regurgitant flow in a Bjork-Shiley Monostrut mechanical heart valve 3 mm away from the valve. The colored contour is the axial velocity, and the vectors represent X and Y velocities. Time = 8 ms after impact.

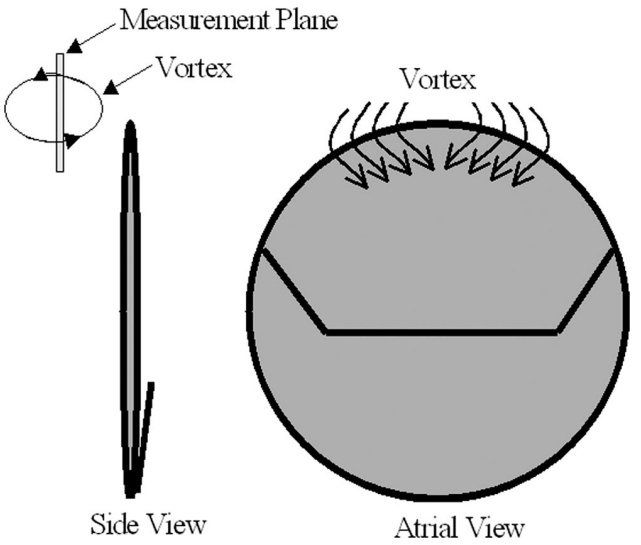

Figure 11. Measurement plane location. Developed vortex is shown by black arrows in front and side views.

flow patterns were seen using PIV along the B-datum and a side cross-sectional view during valve closure and rebound for the BSM.[27]

These results indicate the potential that stable bubbles (mircoembolic signals or HITS) observed with transcranial ultrasound may arise because of the local fluid mechanics near the major orifice side of the BSM MHV. This study provides further insight into the cavitation development during closure and rebound as a result of the more confined regions surrounding the valve. Furthermore, the local fluid mechanics that develops during closure and rebound is highly three-dimensional, and the vortex intensity is driven by the regurgitant jet that develops after rebound.

Conclusion

A modified, single shot MHV chamber with more confined regions near the valve was used to more accurately simulate

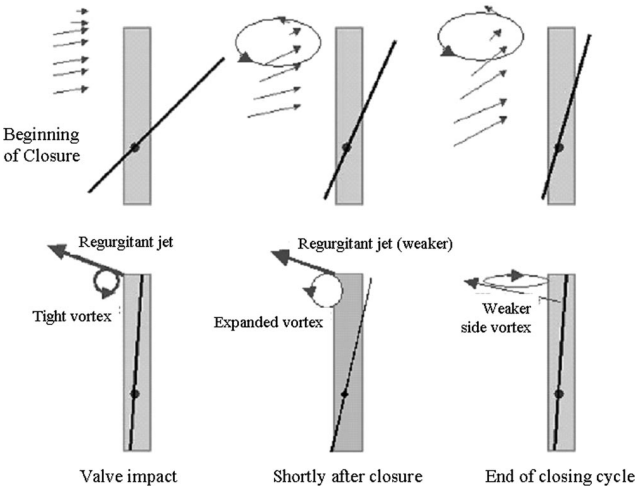

Figure 12. Flow field schematic during the closing cycle.

the flow fields *in vivo* with a BSM MHV. The development of a vortex was illustrated during the closing phase. This vortex, which is strengthened during rebound, has the potential to induce vaporous cavitation, as indicated in previous studies. Because of the presence of nuclei, stable bubbles may develop (potentially causing strokes) as indicated by ultrasound, high intensity transient signals, and neurologic deficits. It is important to understand MHV cavitation to reduce the adverse effects. A limitation of this study is that a higher than normal dP/dt (3,500 mm Hg/s) was used to understand cavitation development.

Acknowledgment

This study was supported by NIH Grant HL 48652.

References

1. Gott VL, Alejo DE, Cameron DE: Mechanical heart valves: 50 years of evolution. *Ann Thorac Surg* 76: S2230–S2239, 2003.
2. Ezekowitz MD: Anticoagulation management of valve replacement patients. *J Heart Valve Dis* 11(Suppl. 1): S56–S60, 2001.
3. Horstkotte D, Schulte H, Bircks W, Strauer BE: Lower intensity anticoagulation therapy results in lower complication rates with the St. Jude Medical prostheses. *J Thorac Cardiovasc Surg* 107: 1136–1145, 1994.
4. Fiore AC, Barner HB, Swartz MT, *et al*: Mitral valve replacement: Randomized trial of St. Jude and Medtronic Hall prostheses. *Ann Thorac Surg* 66: 707–713, 1998.
5. Kafesjian R, Howanec M, Ward GD, Diep L, Wagstaff LS, Rhee R: Cavitation damage of Pyrolytic Carbon in mechanical heart valves. *J Heart Valve Dis* 3: 52–57, 1994.
6. Garrison LA, Lamson TC, Deutsch S, Geselowitz DB, Gaumond RP, Tarbell JM: An in-vitro investigation of prosthetic heart valve cavitation in blood. *J Heart Valve Dis* 3: S8–S24, 1994.
7. Zapanta CM, Stinebring DR, Deutsch S, Geselowitz DB, Tarbell JM: Continuing investigations of in vivo prosthetic heart valve cavitation. *Ann Biomed Eng* 24: S4, 1996.
8. Zapanta CM, Stinebring DR, Sneckenberger DS, *et al*: In vivo observation of cavitation on prosthetic heart valves. *ASAIO J* 42: M550–M555, 1996.
9. Graf T, Reul H, Detlefs C, Wilmes R, Rau G: Causes and formation of cavitation in mechanical heart valves. *J Heart Valve Dis* 3: S49–S64, 1994.
10. Chandran KB, Aluri S: Mechanical valve closing dynamics: Relationship between velocity of closing, pressure transients, and cavitation initiation. *Ann Biomed Engr* 25: 926–938, 1997.
11. Hwang NHC: Cavitation potential of pyrolytic carbon heart valve prostheses: A review and current status. *J Heart Valve Dis* 7: 140–150, 1998.
12. Chandran KB, Lee CS, Chen LD: Pressure field in the vicinity of mechanical valve occluders at the instant of valve closure: Correlation with cavitation initiation. *J Heart Valve Dis* 3: S65–S76, 1994.
13. Zapanta CM, Liszka Jr EG, Lamson TC, *et al*: A method for real-time in vitro observation of cavitation on prosthetic heart valves. *J Biomechanical Engr* 116: 460–468, 1994.
14. Sneckenberger DS, Stinebring DR, Deutsch S, Geselowitz DB, Tarbell JM: Mitral heart valve cavitation in an artificial heart environment. *J Heart Valve Dis* 5: 216–227, 1996.
15. Biancucci BA, Deutsch S, Geselowitz DB, Tarbell JM: In vitro studies of gas bubble formation by mechanical heart valves. *J Heart Valve Dis* 8: 186–196, 1999.
16. Lin H-Y, Biancucci BA, Deutsch S, Fontaine AA, Tarbell JM: Observation and quantification of gas bubble formation on a mechanical heart valve. *J Biomechanical Engr* 122: 304–309, 2000.
17. Bachmann C, Kini V, Deutsch S, Fontaine AA, Tarbell JM: Mechanisms of cavitation and the formation of stable bubbles on the Bjork-Shiley Monostrut prosthetic heart valve. *J Heart Valve Dis* 11: 105–113, 2002.
18. Wu ZJ, Wang Y, Hwang NHC: Occluder closing behavior: A key factor in mechanical heart valve cavitation. *J Heart Valve Dis* 3: 525–534, 1994.
19. Bluestein D, Einav S, Hwang NHC: A squeeze flow phenomenon at the closing of a bileaflet mechanical heart valve prostheses. *J Biomech* 27: 1369–1378, 1994.
20. Makhijani VB, Yang HQ, Singhal AK, Hwang NHC: An experimental-computational analysis of MHV cavitation: Effects of leaflet squeezing and rebound. *J Heart Valve Dis* 3: 535–548, 1994.
21. Grosset DG, Cowburn P, Georgiadis D, Darrgie HJ, Faichney A, Lees KR: Ultrasound detection of cerebral emboli in patients with prosthetic heart valves. *J Heart Valve Dis* 3: 128–132, 1994.
22. Deklunder G, Lecroart JL, Savoye C, Coquet B, Houdas Y: Transcranial high intensity Doppler signals in patients with mechanical heart valve prosthesis: Their relation with abnormal intracavitary echoes. *J Heart Valve Dis* 6: 662–667, 1996.
23. Kleine P, Perthel M, Hasenkam JM, Nygaard H, Hansen SB, Laas J: High-intensity transient signals (HITS) as a parameter for optimum orientation of mechanical aortic valves. *Thorac Cardiov Surg* 48: 360–363, 2000.
24. Meyer JS, Muramatsu K, Shirai T: Cerebral embolism as a cause of stroke and transient ischemic attack. *Echocardiography* 13: 573–577, 1996.
25. Droste DW, Hansberg J, Kemeny V, *et al*: Oxygen inhalation can differentiate gaseous from nongaseous microemboli detected by transcranial Doppler ultrasound. *Stroke* 28: 2453–2456, 1997.
26. Georgiadis D, Wenzel A, Lehmann D, *et al*: Influence of oxygen ventilation on Doppler microembolic signals in patients with artificial heart valves. *Stroke* 28: 2189–2194, 1997.
27. Kini V, Bachmann C, Fontaine AA, Deutsch S, Tarbell JM: Flow visualization in mechanical heart valves: Occluder rebound and cavitation potential. *Ann Biomed Engr* 28: 431–441, 2000.
28. Kini V, Bachmann C, Fontaine AA, Deutsch S, Tarbell JM: Integrating particle image velocimetry and laser Doppler velocimetry measurements of the regurgitant flow field past mechanical heart valves. *Artif Organs* 25: 136–145, 2001.
29. Manning KB, Kini V, Fontaine AA, Deutsch S, Tarbell JM: Regurgitant flow field characteristics of the St. Jude bileaflet mechanical heart valve under physiologic Pulsatile flow using particle image velocimetry. *Artif Organs* 27: 840–846, 2003.
30. He Z, Xi B, Zhu K, Hwang NHC: Mechanisms of mechanical heart valve cavitation: Investigation using a tilting disk valve model. *J Heart Valve Dis* 10: 666–674, 2001.